Supporting Information

3D-Printed pHEMA Materials for Topographical and Biochemical Modulation of Dorsal Root Ganglion Cell Response

Adina Badea[a], *Joselle M. McCracken*[a], *Emily G. Tillmaand*[c], *Mikhail E. Kandel*[d], *Aaron W. Oraham*[a], *Molly B. Mevis*[a], *Stanislav S. Rubakhin*[a], *Gabriel Popescu*[d], *Jonathan V. Sweedler*[a, c] *, *and Ralph G. Nuzzo*[a, b] *

[a] School of Chemical Sciences, [c] Neuroscience Program, [d] Department of Electrical and Computer Engineering, University of Illinois-Urbana Champaign, Urbana, IL 61801, United States of America, and [b] School of Chemical Science and Engineering, KTH Royal Institute of Technology, Stockholm, Sweden

Corresponding Authors

*E-mail: r-nuzzo@illinois.edu, jsweedle@illinois.edu

Supplemental Methods

Reagent List. Poly-D-lysine (PDL, hydrobromide, Mw 30,000-70,000), Bright-Line™ Hemocytometer, Cytosine α-D-arabinofuranoside (AraC), 2-Hydroxyethyl methacrylate monomer (HEMA, 99%, containing 50 ppm monomethyl ether hydroquinone as inhibitor), poly(2-hydroxyethyl) methacrylate (pHEMA, average Mv 1,000,000, powder); and the radical initiator 2,2-Dimethoxy-2-phenylacetophenone (DMPA, 99%), and Bovine Serum Albumin (BSA, powder) were purchased from Sigma-Aldrich. Organic cross-linker ethylene glycol dimethacrylate (EGDMA, 98%, containing 90-110 ppm monomethyl ether hydroquinone as inhibitor) was purchased from Sigma-Aldrich; the inhibitor was removed with a pre-packed column for removing hydroquinone and monomethyl ether hydroquinone (Sigma-Aldrich) and stored away from light at 2-5 °C prior to use. N-Succinimidyl 3-[2-pyridyldithio]-propionate (SPDP) was purchased from ProteoChem, cyc (RGDyC) was purchased from Peptides International, Ac - GCGYGRGDSPG - NH_2 was purchased from AnaSpec, desalting columns were purchased from Fischer Scientific. Embryonic murine fibroblasts (NIH/3T3, CRL-1658) and Dulbecco's Modified Eagle's Medium (DMEM) were purchased from ATCC. Trypan Blue solution, phosphate buffered saline, trypsin-EDTA, Penicillin-Streptomycin (Pen/Strep), NGF 2.5S Native Mouse Protein, Hank's Balanced Salt Solution (HBSS), Neurobasal-A Medium, B-27 serum free supplement, GlutaMAX, 1% Triton X-100 solution, Rhodamine-Phalloidin (R-P) fluorophore, Prolong Gold antifade agent were purchased from Life Technologies, cell culture grade Dimethyl Sulfoxide (DMSO) and Paraformaldehyde solution were purchased from Santa Cruz Biotechnology, Type 2 Collagenase was purchased from Worthington Biochemical, human BDNF was purchased from ProSpec, chicken polyclonal anti-GFAP antibody was purchased from Abcam. 4,6-Diamidino-2-phenylindole dihydrochloride (DAPI) was purchased from

Polysciences Inc. Water used in all experiments was purified using a Milli-Q water purification system (Millipore, Bedford, MA) with resistivity higher than 18MΩ·cm. HEPES buffer was prepared in house and consists of 20 mM HEPES, 115 mM NaCl, 1.2 mM $CaCl_2$, 1.2 mM $MgCl_2$, and 2.4 mM K_2HPO_4 in Milli-Q water. The pH was adjusted to 7.4 using HCl or NaOH. Buffer was stored in the fridge until use and for no longer than 6 weeks. DRG media used for adult rat DRG cell culture consists of Neurobasal A supplemented with 2% B-27 serum free supplement, 0.25% GlutaMAX, 1% Penicillin/Streptomycin, 0.05% murine neural growth factor (NGF), and 0.05% human brain-derived neurotrophic factor (BDNF). Cytosine arabinoside (AraC) is added up to a final concentration of 0.3 µM for glial proliferation inhibition.

Quantification of PDL Modifications. A trypan blue assay was previously documented as a method for quantifying poly-lysine concentrations.[1] Trypan blue is a highly negatively charged dye which interacts with the cationic PDL to form quantitative precipitation. It has a maximum absorption at 580 nm, so precipitation causes a decrease in signal in that region proportional to

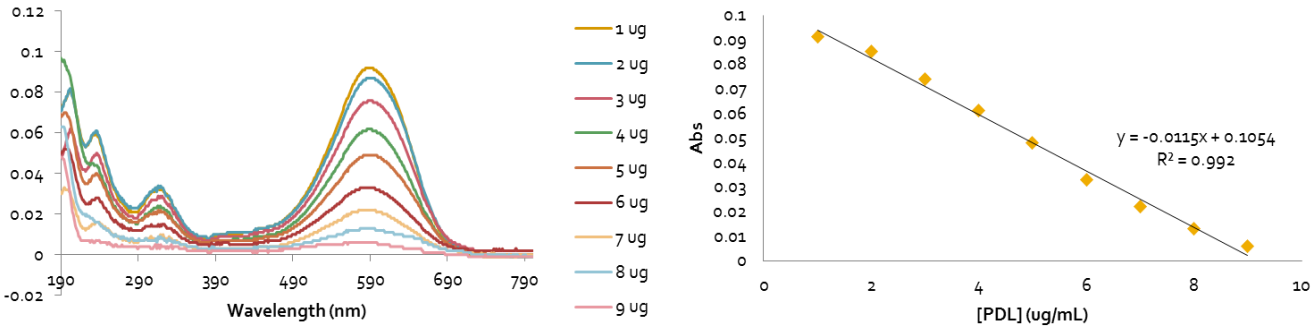

Figure S1. Trypan blue assay and calibration curve

the amount of PDL in solution. As the poly-lysine used in that study had a different molecular weight range (15-30 kDa) than the PDL used in our studies (30-70 kDa), a new calibration curve had to be determined (Fig. S1).

Coupled with the specific absorption of the byproduct, pyridine-2-thione, released in stoichiometric amounts with the degree of RGD crosslinked to PDL, this method allowed the quantification of RGD to PDL ratios using the following equation:

$$\frac{\Delta A}{8.08 \times 10^3\ M^{-1}cm^{-1}} \times \frac{MW\ of\ Protein}{\frac{mg}{mL}of\ Protein} = moles\ of\ SPDP\ per\ mole\ of\ Protein$$

ΔA is the change in absorption after the peptide addition, and 8.08×10^3 $M^{-1}cm^{-1}$ is the molar extinction coefficient for pyridine-2-thione at 343 nm. Typical spectra of RGD-PDL types 1-4 and of a set of control reactions lacking SPDP to test whether the peptides are covalently attaching or just aggregating with the protein was run, are shown in Fig. S2.

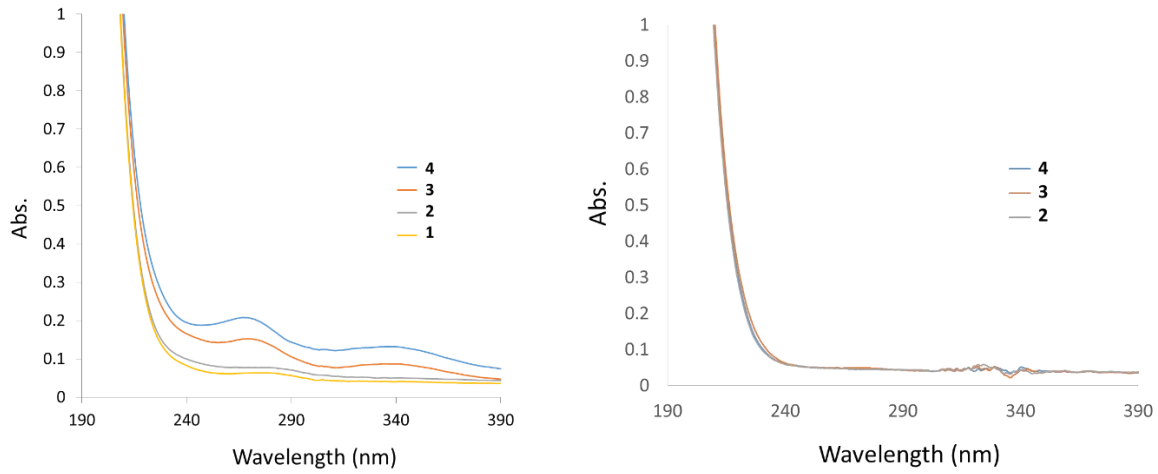

Figure S2. UV-Vis spectra of cycRGD-PDL 1-4 (left) and of control reactins for cycRGD-PDL 2-4 (right)

Fabrication of pHEMA Films. The pHEMA solution formulation is 5.7 wt% pHEMA (300,000 Mw), 2.2 wt% pHEMA (1,000,000 Mw), 8.8 wt% HEMA, 5.4 wt% H2O, 0.4 wt% EGDMA, 0.2 wt% DMPA, 38.5 wt% ethylene glycol, and 38.5 wt% ethanol. 25 mm diameter round 1.5H high precision glass coverslips (Azer Scientific) were cleaned with ethanol and dried under flowing nitrogen. The slides were then spin coated with the ink at 900 rpm for 90s x 3. The

coated slides were then exposed to UV light (OmniCure S2000, Exfo) for ~3.5 h. The sterilized slides were then either used immediately, or stored in a sterile laminar flow hood until use.

Preparation of pHH (pHEMA) ink. The standard ink formulation is 25 wt% pHEMA (300,000 Mw), 10 wt% pHEMA (1,000,000 Mw), 40 wt% HEMA, 23.5 wt% H2O, 1 wt% EGDMA, and 0.5 wt% DMPA. MilliQ water, HEMA, EGDMA, and DMPA are combined and stirred until the DMPA dissolves. The pHEMA is added and the mixture is stirred for 1-2 weeks until a homogenous solution forms. Manual mechanical agitation is found to be an effective way to accelerate the homogenization process. For inks that contain RGD-PDL, 0.5 mL of 1.4 mg/mL of the modified peptide solution is added to 3.4 g pHEMA/HEMA (pHH) ink such that the final aqueous weight fraction was 35%. This is then homogenized, yielding a printable ink with moderately lower viscosity.

Micro-pattern and 3D Scaffold Fabrication. G-Code programming language was used for generating diverse scaffold patterns. Aluminum plates manufactured at the Physics-MRL Machine Shop were mounted onto the axial stage, and a TangoGray FLX950 rubber syringe spacer/adaptor was printed at the MechSE Rapid Prototype Lab on the Eden 350 (Objet Geometries, Ltd.) for axially-mounting syringe barrels. An Ultimus V High Precision dispenser (Nordson EFD) was used for positive-pressure controlled printing. For pHEMA/HEMA gel printing, generally a 30 μm pre-pulled glass pipette tip print-head (World Precision Instruments Inc.) that had been sputter-coated to opacity with Au/Pd to prevent ink drying at the orienting tip was used, in combination with 3cc amber light block syringe barrels. Relative printing pressure

and print speed were adjusted for microscopic differences in printheads and for ink viscosity differences such that scaffold filament spacing and feature resolution was preserved. An IDS USB 3.0 C-Mount Camera with a color CMOS sensor was mounted with a 1.5× Navitar Attachment Lens and a 2.0× Precise Eye Navitar Adaptor Lens (1stVision Inc.) for high magnification imaging of scaffold. The camera was mounted to the axial stage with a 10.9" holding arm (Noga) to allow for synchronous motion of the camera and the printhead. Ambient lighting is supplied to the printing area with a 6 Watt LED Dual Goose-neck Illuminator (AmScope).

NIH/3T3 Fibroblasts Seeding and Culture. Cells are grown in a humidified incubator at 37 ºC with 5% CO_2. At 60-80% confluence, fibroblasts were incubated with 3 mL Trypsin (Life Technologies) for 12 min to achieve complete cell detachment. Resulting solutions were neutralized with 4 mL of complete media and flasks were rinsed with 3 mL Dulbecco's Phosphate Buffered Saline to completely transfer cells prior to centrifugation. Cells were pelleted from solution and re-suspended in complete medium prior to scaffold seeding. Hydrogel scaffolds were rinsed with EtOH then sealed onto a petri dish with a circumferential thermal adhesive ring. These assemblies are sterilized prior to cell plating, through 300 Watt UV light exposure in the laminar flow hood for 30 min. Scaffolds are immersed in a 100 µg/ml PDL or RGD-modified PDL solution for 60 min prior to seeding. Cells are plated onto the scaffolds at approximately 0.5×10^6 cells/ml and allowed to proliferate for approximately 48 h.

NIH/3T3 Fibroblasts Fluorescence Imaging – Actin/Nuclei Staining. After 2 d in culture, NIH/3T3 fibroblasts are rinsed 3x with PBS, immersed in 4% paraformaldehyde at ambient conditions (23-25 °C) for 10 min and then rinsed again with PBS. A PBS/0.25% Triton X-100 is placed on the cells for 3 min to permeate their membranes and then the samples are rinsed again with PBS. The cells are incubated in 1% bovine serum albumin (BSA, Sigma Aldrich) in PBS for 10 min to reduce non-specific binding of fluorescent stains. The cells are then incubated for 20 min in a rhodamine-phalloidin (Invitrogen Molecular Probes) solution diluted 1:200 in 1% BSA solution, and again rinsed with PBS. Finally, the samples are incubated with 0.002% DAPI in PBS (4', 6-diamidino-2-phenylindole, Invitrogen Molecular Probes) for 1 min and rinsed with milliQ water. To prepare for imaging, thermal adhesive rings were removed from scaffolds, permitting separation of the scaffolds from the petri dish, and portions of the samples which were not targeted by imaging were wiped with EtOH. Fluoro-gel (EMS Acquisition Corp.) liquid mounting medium was applied to the scaffolds to prevent photo-bleaching and to protect the integrity of scaffold filaments. 25 mm diameter, round, 1.5H high precision coverslips (Azer Scientific) were then placed over the mounting medium. Samples were stored away from light at 4°C until immediately prior to imaging.

Fiji Quantification of NIH/3T3 Fibroblast Response to RGD-PDL Surface Treatments. The custom Fiji (ImageJ2) software package was used for semi-automated cell counting. To assist with quantification, the blue (DAPI) channel of the fluorescence images of each surface treatment and control was used. Briefly, an intensity threshold that allowed visibility of all cell nuclei was set to select cells and the ‘analyze’ particle tool was used with default selection of object size and shape during counting. To account for the lack of uniformity of cell growth on

scaffolds, six 1.6 mm × 1.6 mm tiles within each culture condition studied were selected for manual cell counts using the polygon selection tool.

Adult Rat DRG Isolation. All work with live animals was performed in full compliance with local and federal guidelines for the humane care and treatment of animals and in accordance with approved by the University of Illinois at Urbana-Champaign IACUC animal use protocol. Adult Sprague-Dawley male rats were quickly decapitated using a sharp guillotine. Spine vertebrae were surgically cut on both side between pedicle and lamina in the area of the facet of superior articular process. This cut exposed the spinal cord which was removed. Additional cuts on sides and in the middle of the ventral portion of the vertebral column created two chains of vertebra pieces with easily visualized DRGs. DRGs were removed using fine forceps and placed into the Hibernate A solution (Life Technologies) located on ice.

MATLAB Quantification of Cell Network Development on Scaffolds. DRG cell culture growth and surface coverage on substrates and scaffolds were quantified in MATLAB post micrograph processing and analysis conducted in Fiji (ImageJ2). Digital masks were applied to the raw DRG cell culture images to separate the scaffold filament areas and the substrate surface areas. Resulting images were converted to 8bit grayscale and the contrast and brightness were adjusted, including background subtraction, for each image such that neuronal outgrowth was defined by black pixels and non-neuronal growth was defined by white and gray pixels. Images were imported as matrices into MatLab software and the pixel counts were summed in each case. The black pixel counts of masked adjusted neuron images were then compared to the pixel counts of the image masks only to calculate the fractional surface area coverage on both scaffold surfaces and substrate surfaces independently. 12-40 individual images were evaluated for each

experiment data point. Each image series spanned multiple scaffold geometries (generally 3) and multiple separate cultured samples (2-3). Separate animal experiments with 5-12 technical replicates were performed and analyzed for all experimental data points.

Immunocytochemistry–Neuronal extensions (MAP2)/Glia (GFAP)/Nuclei Staining. After 7 d in culture, neurons were rinsed 3 times with PBS (37 °C), immersed in 4% paraformaldehyde (37 °C) at ambient temperature (23-25 °C) for 20 min and then rinsed again with PBS, five times (last time for 5 min on a shaking board). A PBS solution containing 0.25% Triton X-100 was added to the samples for 10 min to permeabilize cellular membranes, before rinsing again with PBS five times. The samples were incubated in a 5% NGS (Normal Goat Serum) for 30 min before rinsing again with PBS five times. The samples were then exposed to primary rabbit anti-MAP2 antibody at a 1:1,000 dilution at 4 ºC overnight and then rinsed five times with PBS. Next, the samples were exposed to primary chicken anti-GFAP (1:1,000 dilution) antibody at room temp for 1 h and then rinsed five times with PBS. Secondary Alexa 594 anti-rabbit and Alexa 488 anti-chicken IgG antibodies (1:200) are added to the samples, which were allowed to incubate for 1 h (23-25 °C). The samples were then rinsed with PBS five times. Finally, the samples were incubated with 0.002% DAPI in PBS for 1 minute and rinsed with deionized water 30 s - 1 min. The samples were covered with 2-3 drops of antifade mounting media and a coverslip was set on top of the mounted sample.

Confocal Fluorescence Imaging. Tiled images of the entire scaffold were obtained using the 10× objective, which were composed of either 2 × 2 tiles (927 μm × 927 μm) or 4 × 4 tiles (1270 μm

× 1270 μm), depending on the scaffold architecture. These 10× magnification images required no immersion medium and were taken with an EC Plan-Neofluar NA=0.3. In addition, single-frame and 2 × 2 tiled images (250 μm × 250 μm) were captured using a 40× objective for data analysis. The 40× magnification images were taken in Zeiss Immersol 518 immersion medium with refractive index ne=1.518 at 23°C. Oversampling for all images was at least 2× as dictated by Nyquist sampling. Pinhole diameters for all images ranged from 1-2 AU, with most measurements performed at approximately 1.6 AU. 20% tile overlap and online stitching permitted high resolution large-area imaging of scaffold structures of interest. Confocal *z*-stacks were reconstructed using ImageJ software.

Quantification of the Association between Neural and Glial Extension Networks. Representative fluorescence micrographs of DRG cultures were selected for a scaffold and substrate region. Volumetric surface rendering of both images was performed on the Zeiss ZEN native software with all parameters kept constant except for Threshold values, which were set to the minimum value at which no bandpass fluorescence noise was detected. The resulting image channels were combined in MatLab software such that nuclei, high association (green and red channel overlap) regions, low association (green or red channel only) regions, and signal-free regions, were categorized with specific grayscale values. Four representative nuclei were selected from high association and low association regions for both scaffold and substrate images, and 20-μm plot profiles were drawn through the lateral axes of each nucleus. From fluorescence peaks in plot profiles, the degree of association between green glial and red neuronal signals was quantified by measuring their respective distance from the nucleus.

Statistical Analyses. The values of the NIH/3T3 Fibroblast cell densities and DRG cell coverage fractions were expressed as Mean ± Standard Deviation (SD). Using OriginPro version 8.6 (OriginLab Corp., Northampton, MA, USA), an analysis of variance (ANOVA) was performed. When appropriate main effects were detected, Tukey's post-hoc (for unequal n) tests were used to make pair-wise comparisons (α set to $p < 0.05$). The Tukey mean comparison tables can be found at the end of the Supporting Information file.

Long Term Imaging and Image Analysis with SLIM. Quantitative phase images were acquired using a Zeiss Z1 microscope coupled to a SLIM module (CellVista SLIM Pro, PhiOptics Inc.). We monitored two volumes of (17.5 mm) × (17.5 mm) × (0.5 mm) over a period of 128.5 h with a 10×/0.3 objective. The large volumes were visualized using the TrakEM2 plugin for ImageJ. To characterize mass transport on the 3D scaffolds, we used *Dispersion-relation phase spectroscopy* to obtain spatial scales of the corresponding cell behavior in the form of a spatial frequency range ("start, "end" spatial scale), methodology previously reported.[2] Here the diffusion and advection coefficients are understood to be the degrees of passive and active transport, respectively. To compare between conditions, we looked at the mass transport along the XY, XZ, and YZ planes (also known as "transverse", "sagittal", "coronal") and the radial averaged composite. Due to the non-gaussian distribution of diffusion/advection spread coefficients, we used the Mann–Whitney U test for statistical significance. It is understood that distributions are different when the test scores fall below a 0.05 confidence threshold, with a score above 0.05 indicating that there is no statistically significant difference between the distributions.

References

1. Grotzky, A., Manaka, Y., Fornera, S., Willeke, M., Walde. P. Quantification of α-polylysine: a comparison of four UV/Vis spectrophotometric methods. *Anal. Methods*, **2010**, *2*, 1448;

2. Kandel, M. E., Fernandes, D., Taylor, A. M., Shakir, H., Best-Popescu, C., Popescu, G. Three-dimensional intracellular transport in neuron bodies and neurites investigated by label-free dispersion-relation phase spectroscopy. *Cytometry Part A* **2017**, DOI: 10.1002/cyto.a.23081.

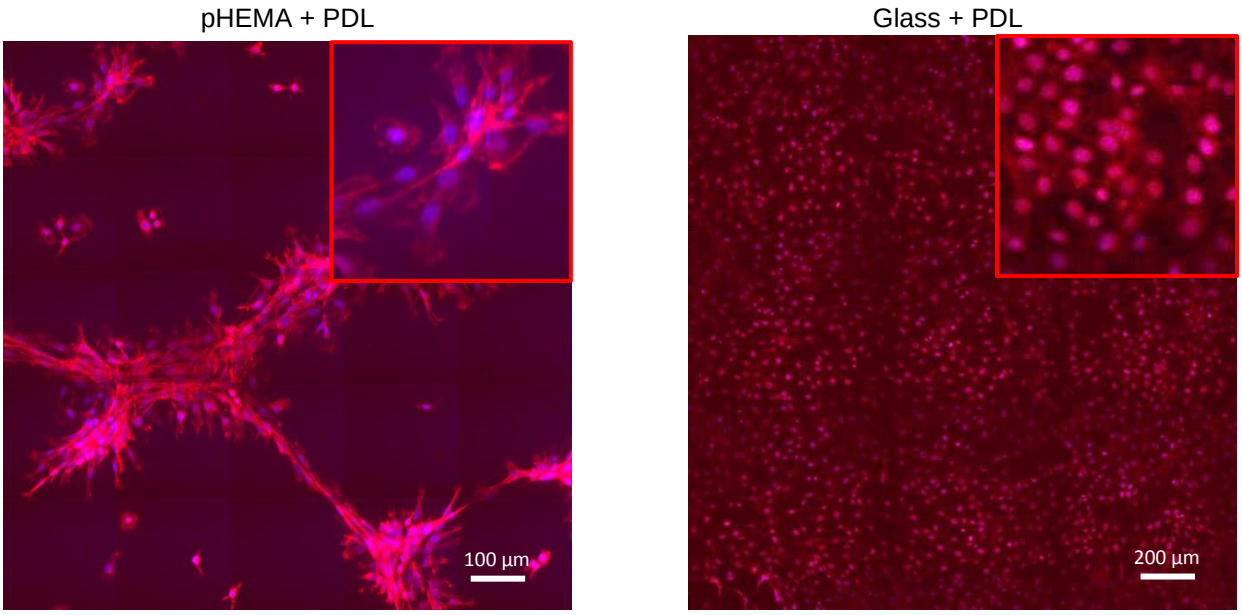

Figure S3. **Control Experiments for the Biocompatibility Assessment of RGD-Modified PDL Surface Treatments.** CFM Images of NIH/3T3 murine fibroblasts on pHEMA (left, 400× magnification) and glass (right, 200× magnification) with PDL as a surface treatment. Actin filaments stained with rhodamine-phalloidin (red), nuclei stained with DAPI (blue). Insets: cell morphology details.

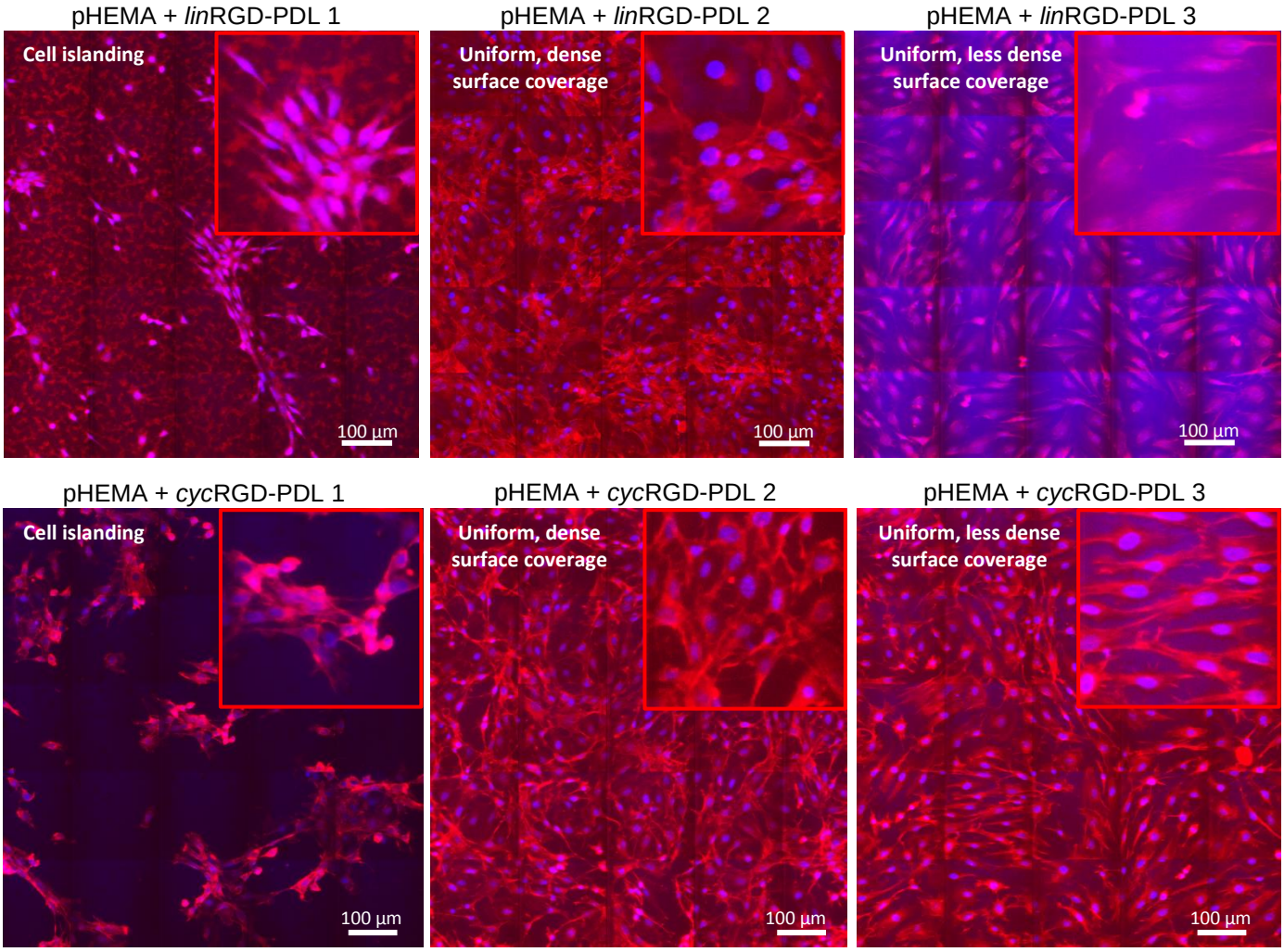

Figure S4. **Complete Experiment Series Showing Fibroblast Response to RGD-PDL Surface Treatments.** CFM Images of NIH/3T3 fibroblasts on different surface treatments 24 h after seeding. Actin filaments stained with rhodamine-phalloidin (red). Insets: cell morphology details.

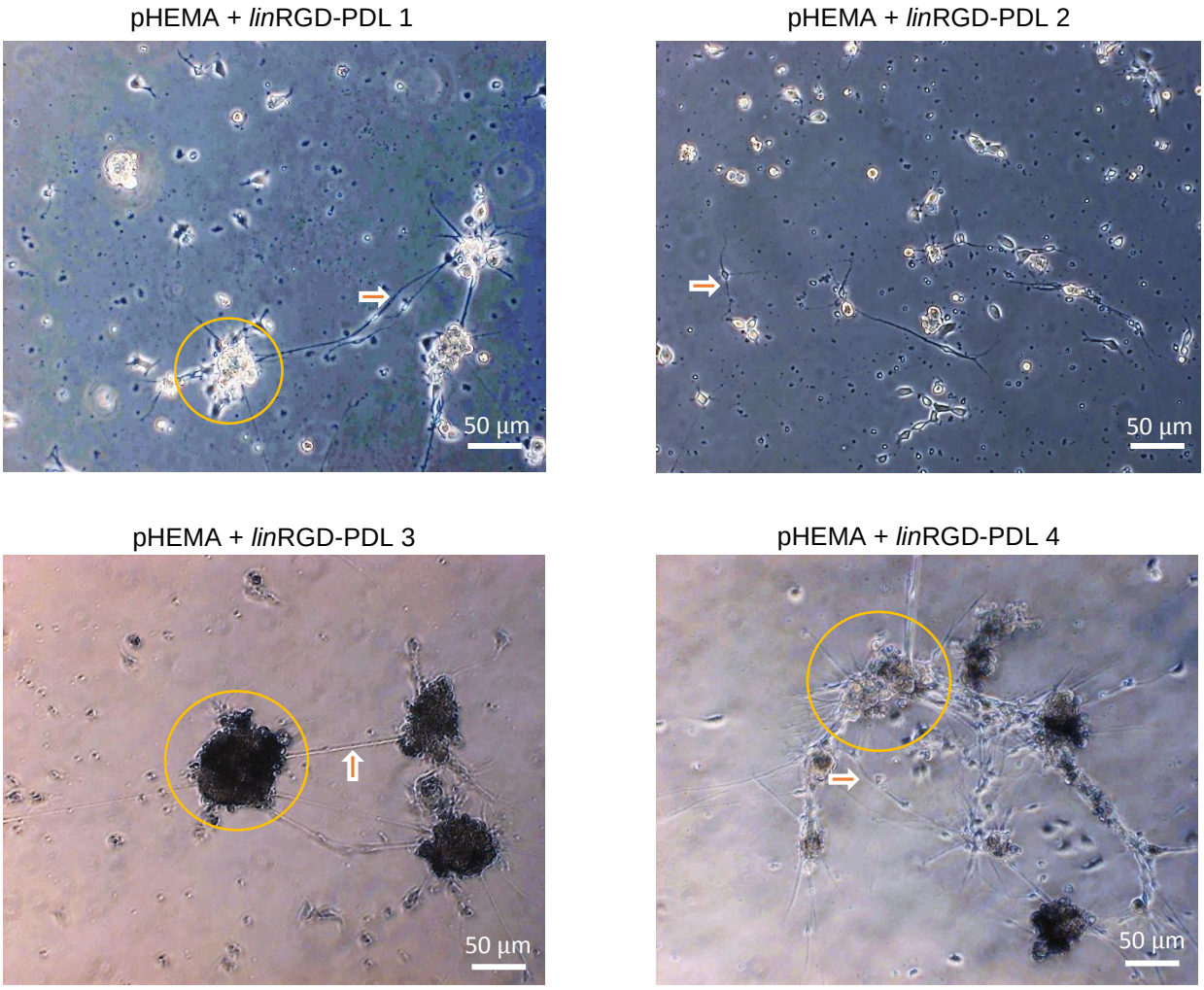

Figure S5. Evaluation of RGD-Modified PDL Surface Treatment Using DRG Cell Culture. Inverted light microscope images of primary rat DRG cells cultured on substrates with different surface treatments after ~9 days in culture. The cell terminals are dark and elongated (arrows). Cell bodies clustered in yellow/orange/brown formations (orange circles).

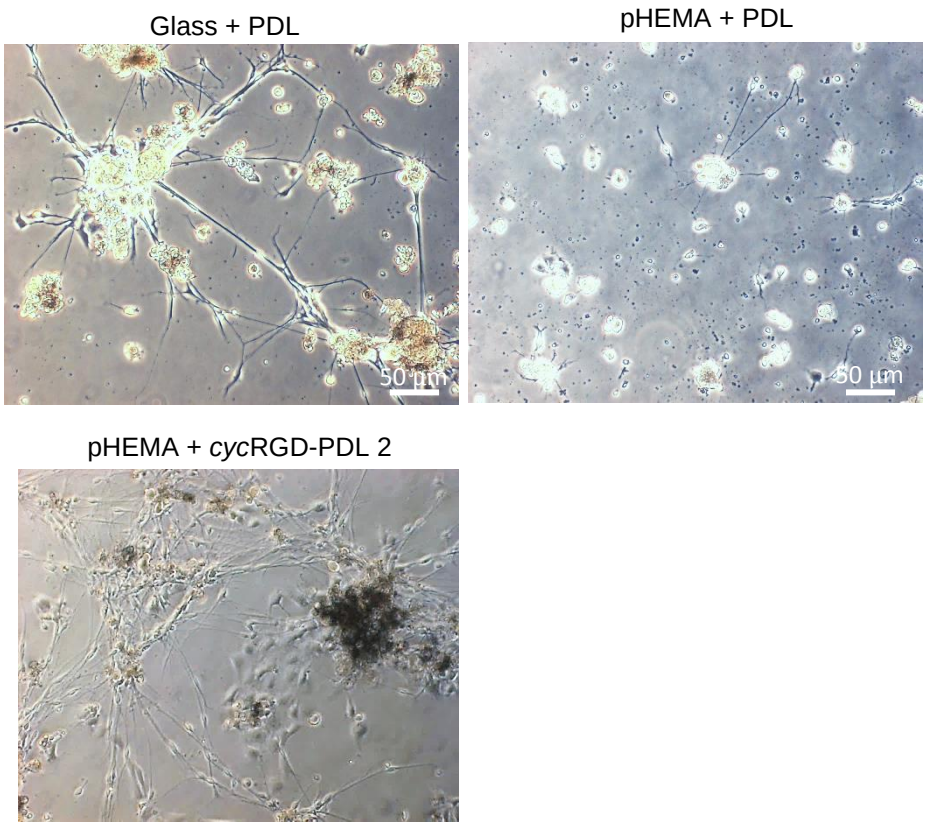

Figure S6. **Evaluation of RGD-Modified PDL Surface Treatment Using DRG Cell Culture.** Inverted light microscope images of primary rat DRG cells cultured on substrates with different surface treatments after ~9 days in culture.

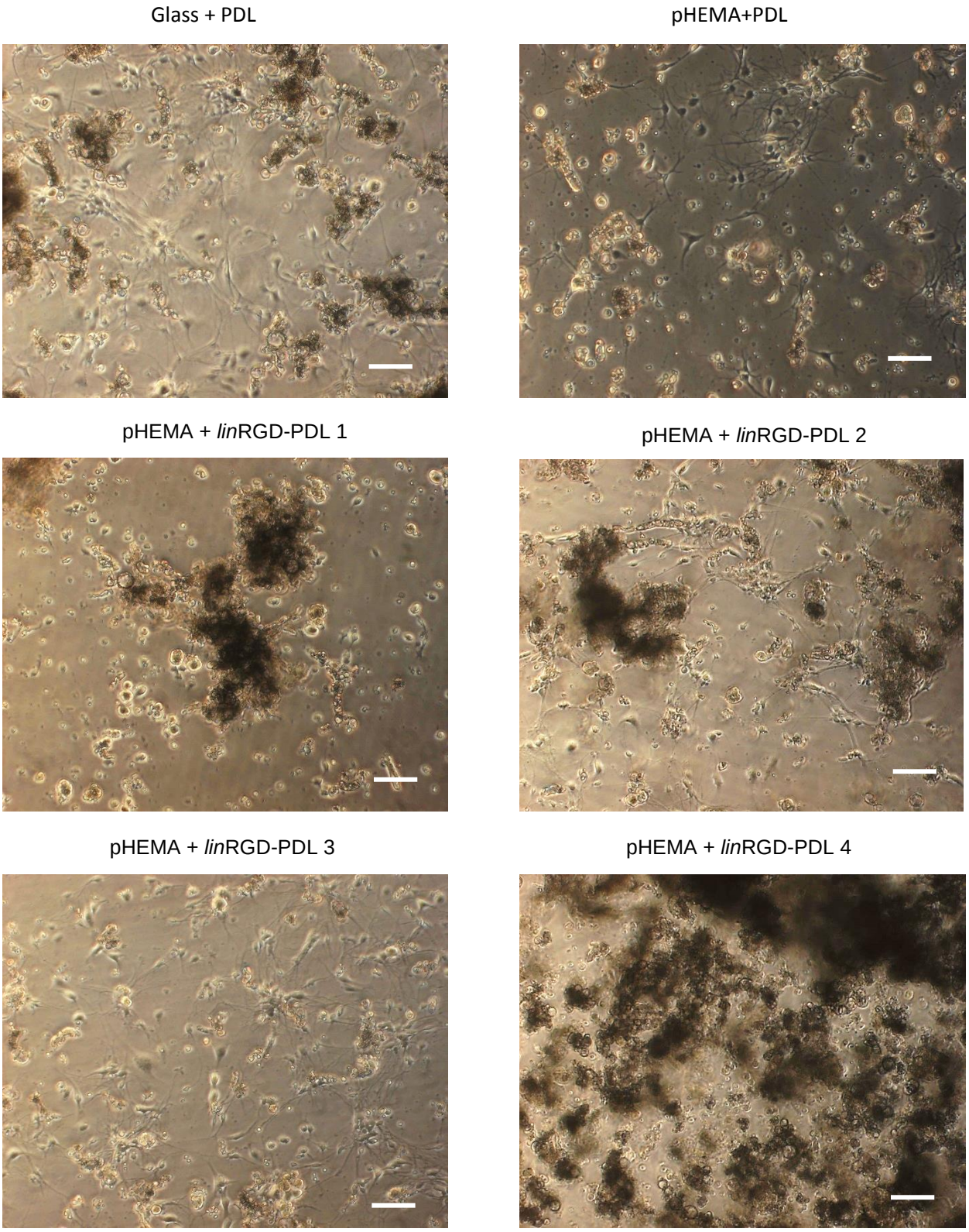

Figure S7. **Time-lapse Images of DRG Cells on RGD-Modified PDL-Treated Surfaces.** Inverted light microscope images of primary rat DRG cells cultured on substrates with different surface treatments after 4 days in culture. Scale bar 50 µm.

pHEMA + *cyc*RGD-PDL 1

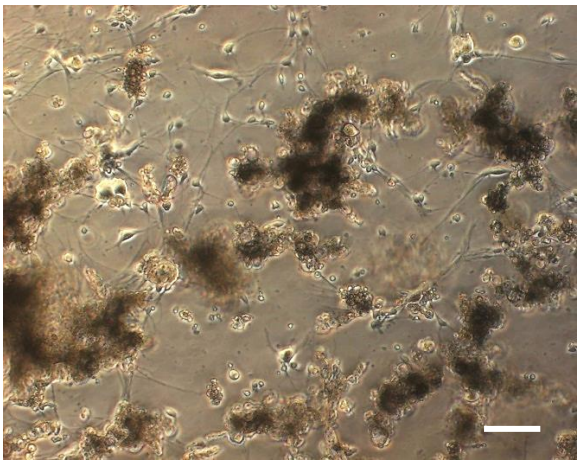

pHEMA + *cyc*RGD-PDL 2

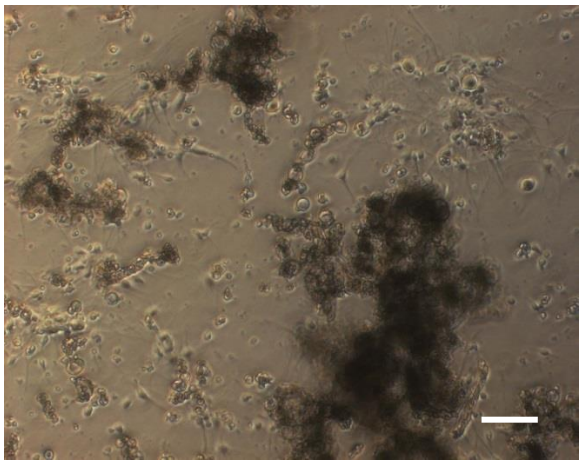

pHEMA + *cyc*RGD-PDL 3

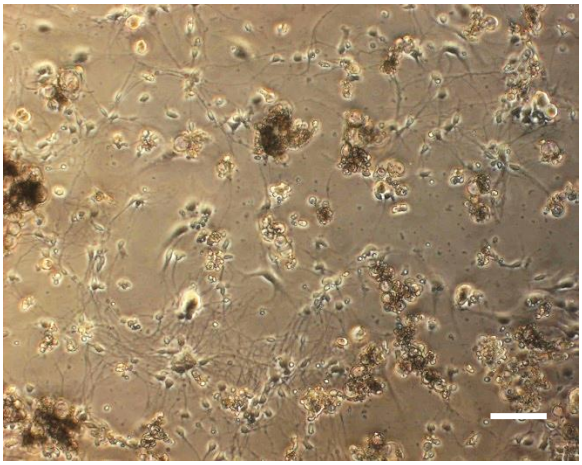

pHEMA + *cyc*RGD-PDL 4

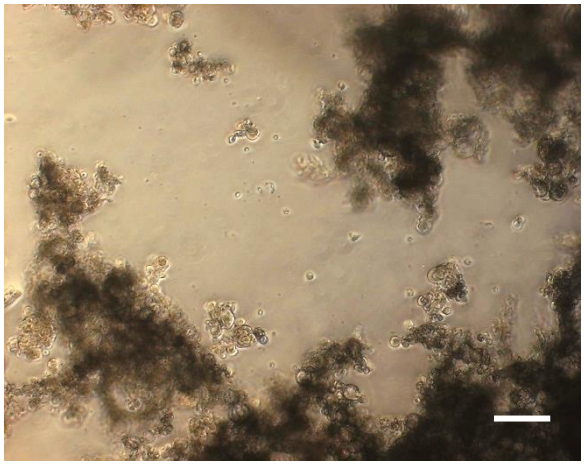

Figure S8. **Time-lapse Images of DRG Cells on RGD-Modified PDL-Treated Surfaces.** Inverted light microscope images of primary rat DRG cells cultured on substrates with different surface treatments after 4 days in culture. Scale bar 50 µm.

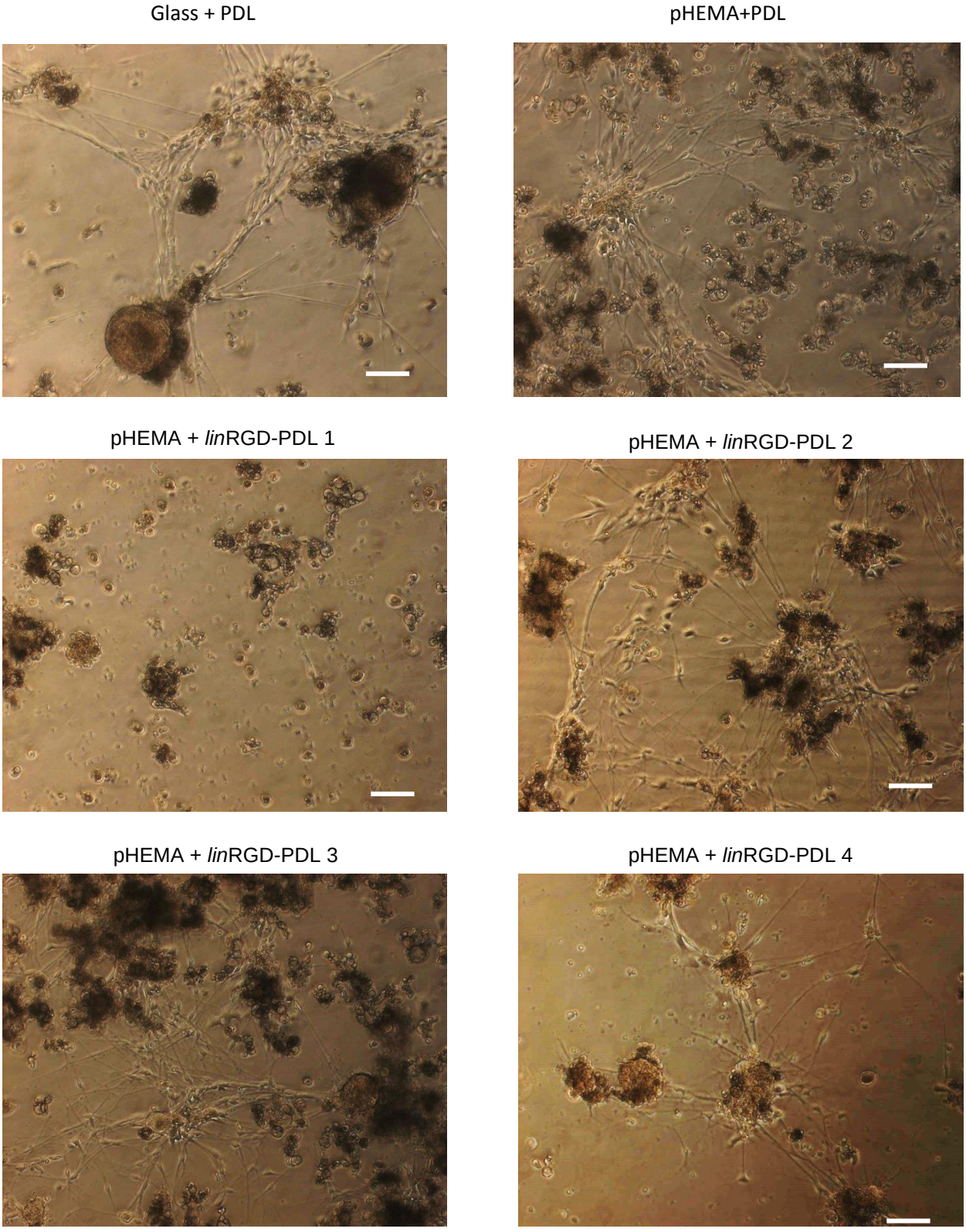

Figure S9. **Time-lapse Images of DRG Cells on RGD-Modified PDL-Treated Surfaces.** Inverted light microscope images of primary rat DRG cells cultured on substrates with different surface treatments after 10 days in culture. Scale bar 50 µm.

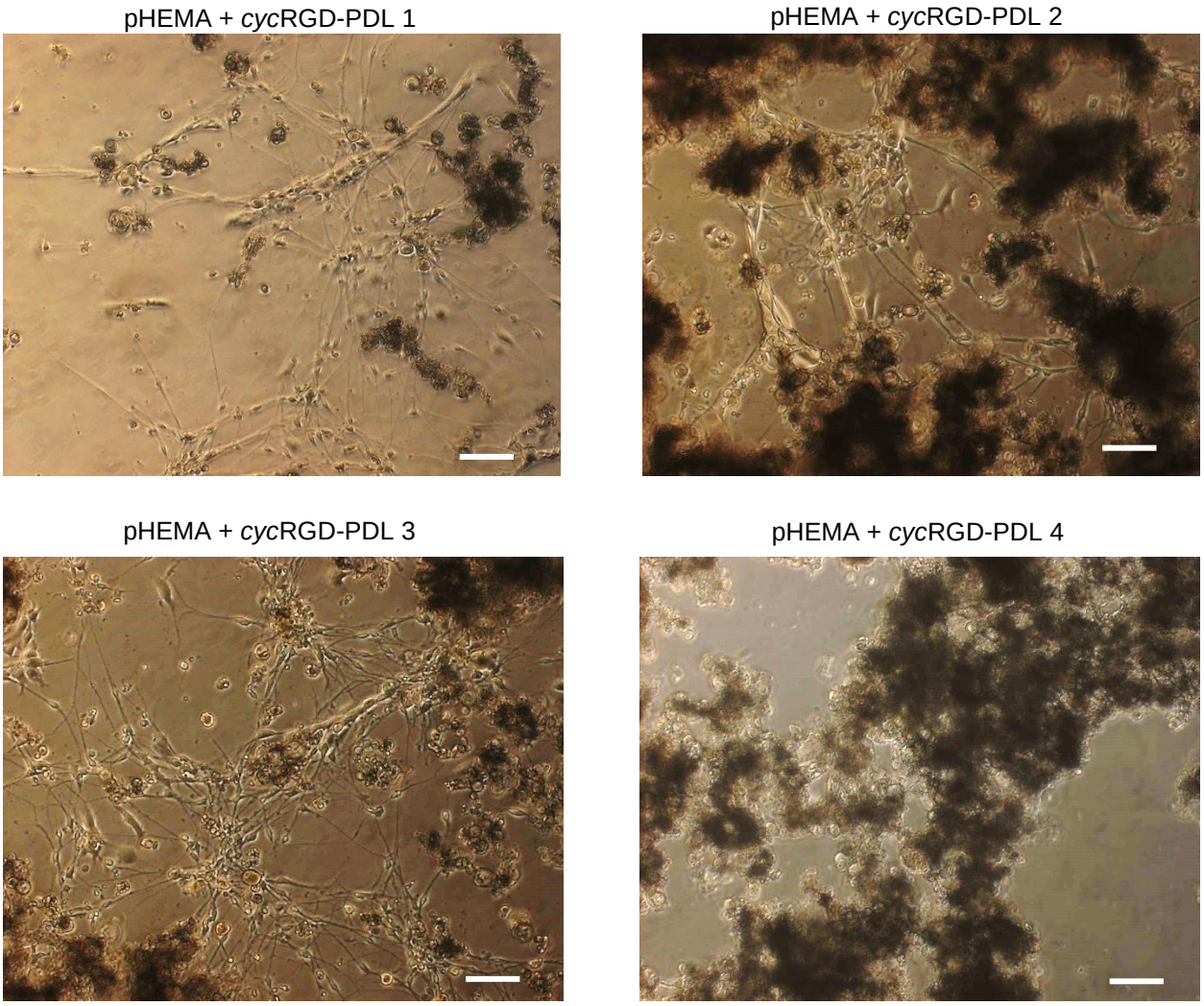

Figure S10. **Time-lapse Images of DRG Cells on RGD-Modified PDL-Treated Surfaces.** Inverted light microscope images of primary rat DRG cells cultured on substrates with different surface treatments after 10 days in culture. Scale bar 50 µm.

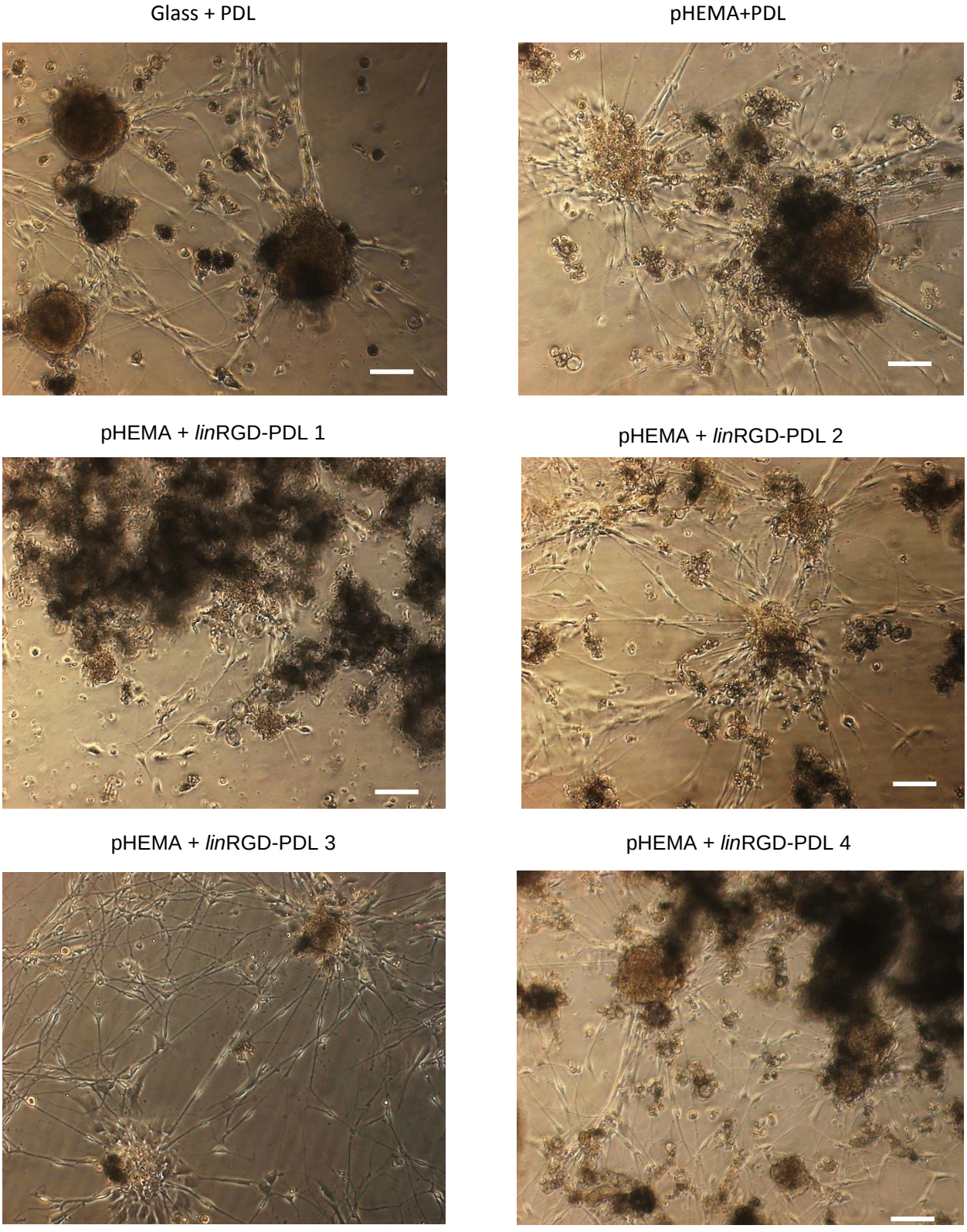

Figure S11. **Time-lapse Images of DRG Cells on RGD-Modified PDL-Treated Surfaces.** Inverted light microscope images of primary rat DRG cells cultured on substrates with different surface treatments after 14 days in culture. Scale bar 50 µm.

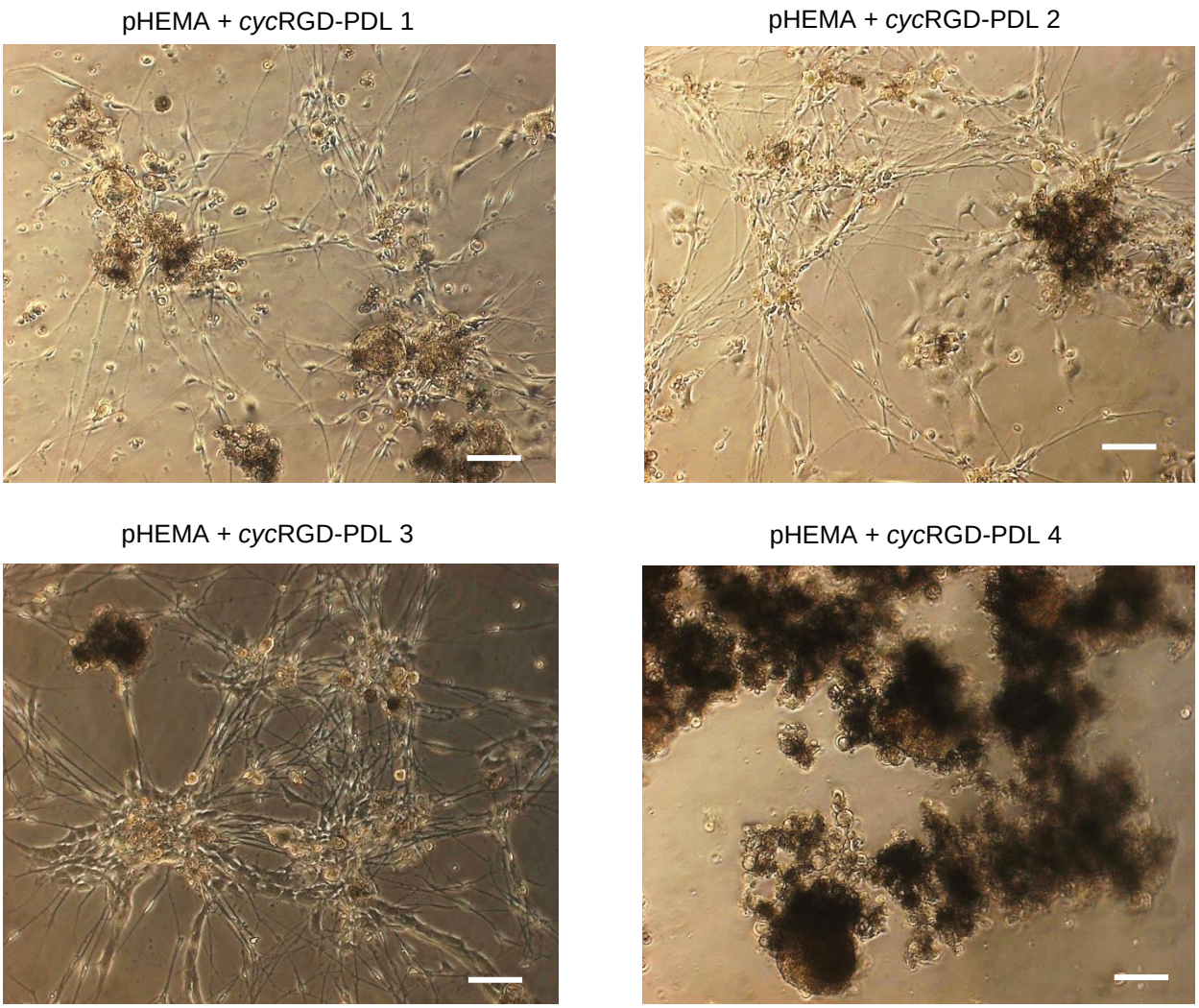

Figure S12. **Time-lapse Images of DRG Cells on RGD-Modified PDL-Treated Surfaces.** Inverted light microscope images of primary rat DRG cells cultured on substrates with different surface treatments after 14 days in culture. Scale bar 50 µm.

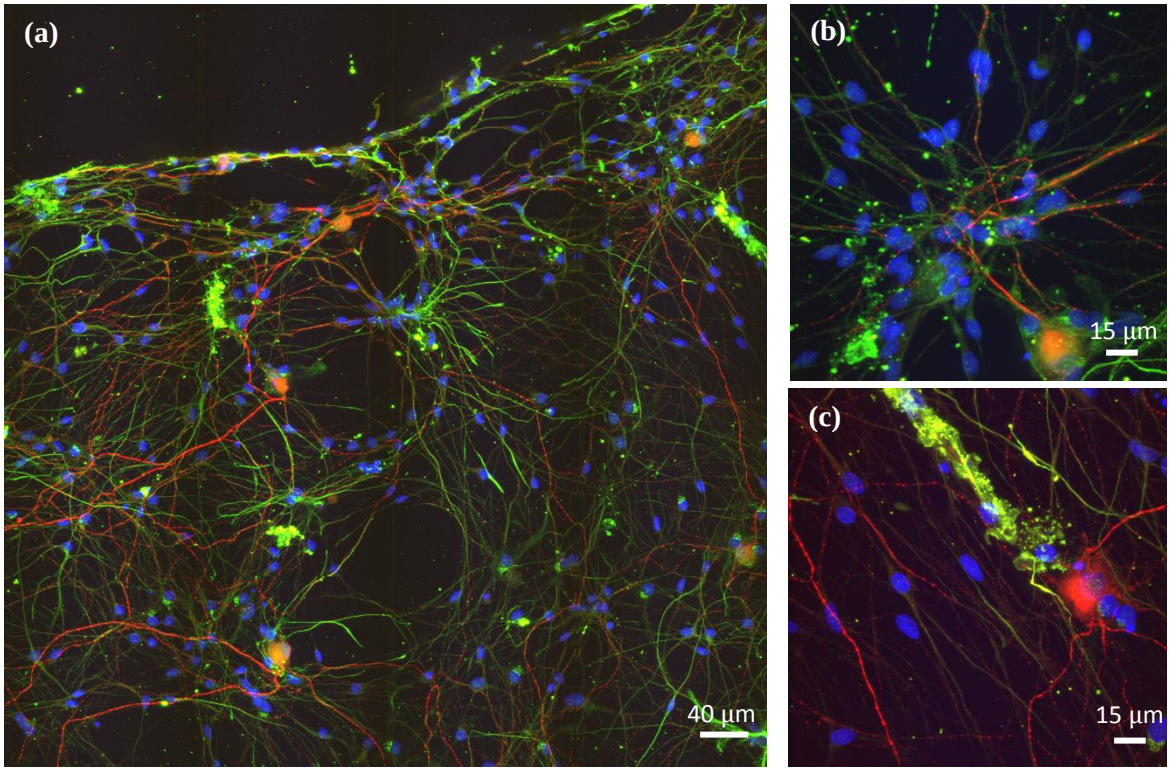

Figure S13. **CFM Images of DRG Cell Networks.** Confocal fluorescence micrographs of primary rat DRG cells cultured on glass slides with *cyc*RGD-PDL 3 surface treatment. Staining marks: nuclei (DAPI, blue), neurons (MAP2, red) and glia (GFAP, green). (b) and (c) show zoomed-in regions presenting cell clusters.

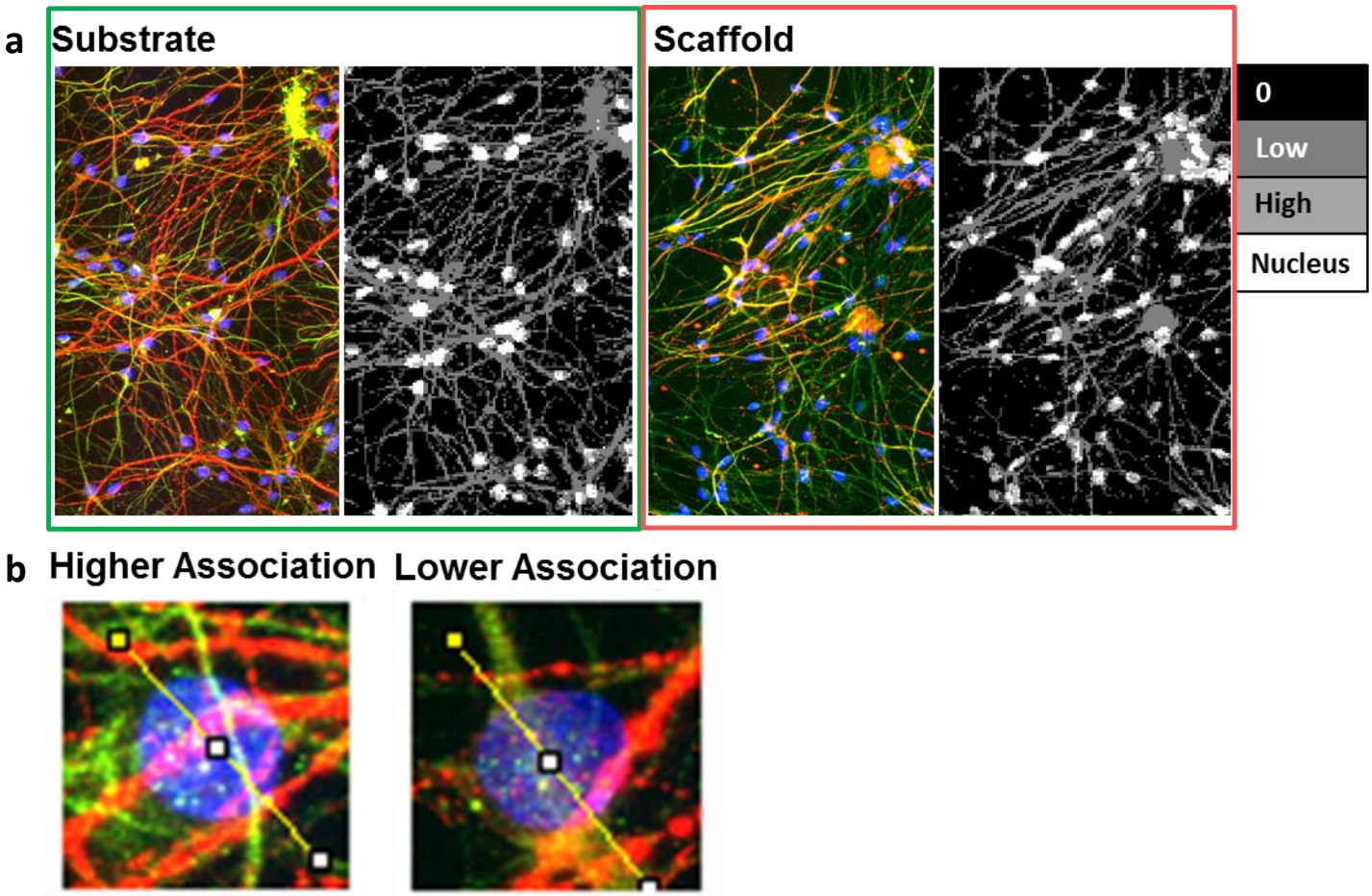

Figure S14. **Glia-Neurons Association Quantification Algorithm.** (a) The color channels of the original confocal fluorescence micrographs are adjusted to reflect degree of overlap of green (corresponding to glia) and red (corresponding to neurons) signals. (b) The distances between the two signals are measured along the lateral axis of the nuclei to which they are closest. Two situations are taken into account: high association between signals, and low association.

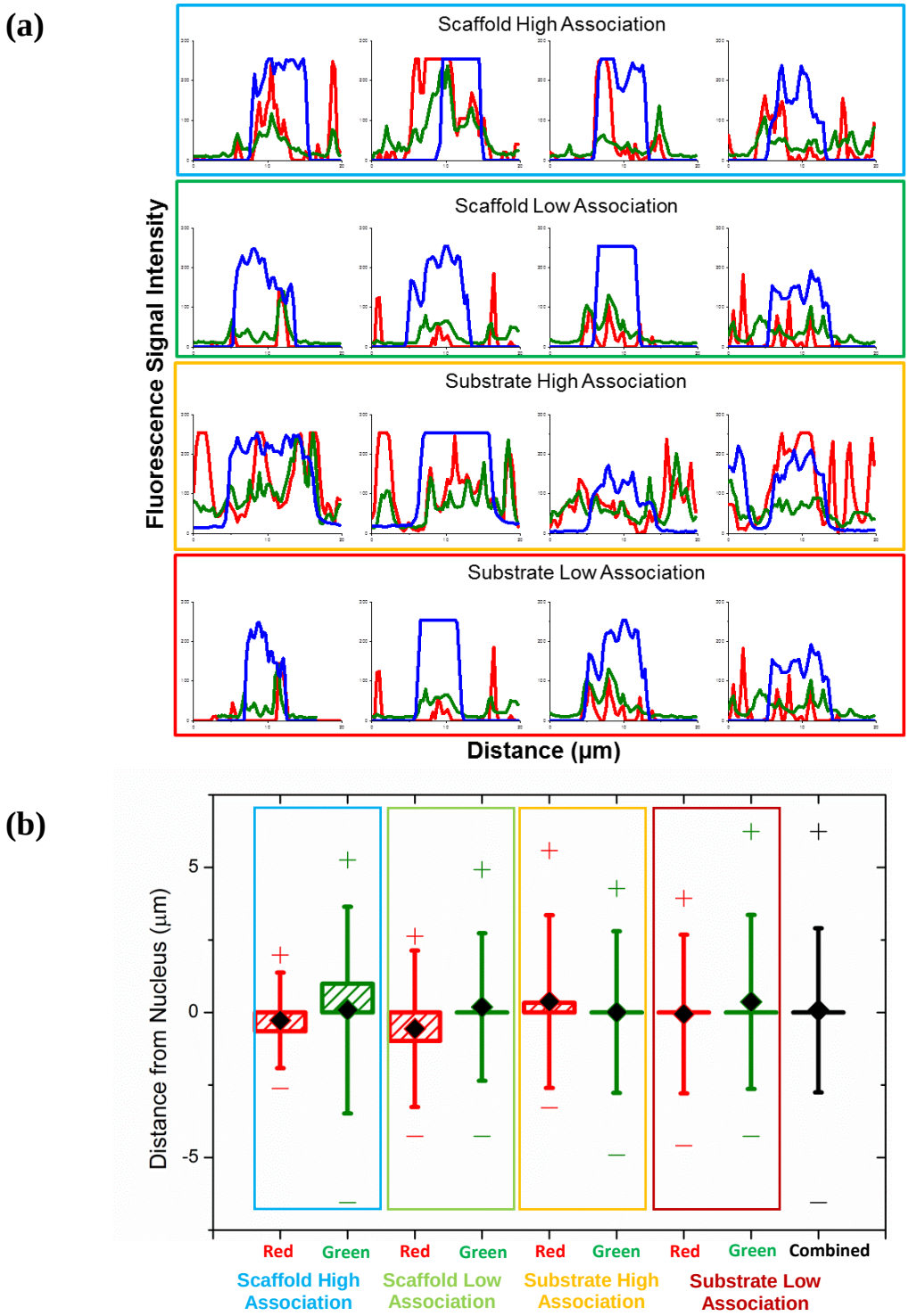

Figure S15. **Glia-Neurons Association Quantification.** (a) Signal intensity profiles of all three color channels of the original confocal fluorescence micrographs corresponding to 4 nuclei in each situation identified in Fig. S13. (b) Box and whisker plots corresponding to the distances between the signals of the two channels with respect to the nuclei to which they are closest. The combined plot shows the distance between the red and green signals across all four situations. The black diamonds represent averages and the error bars represent standard deviations.

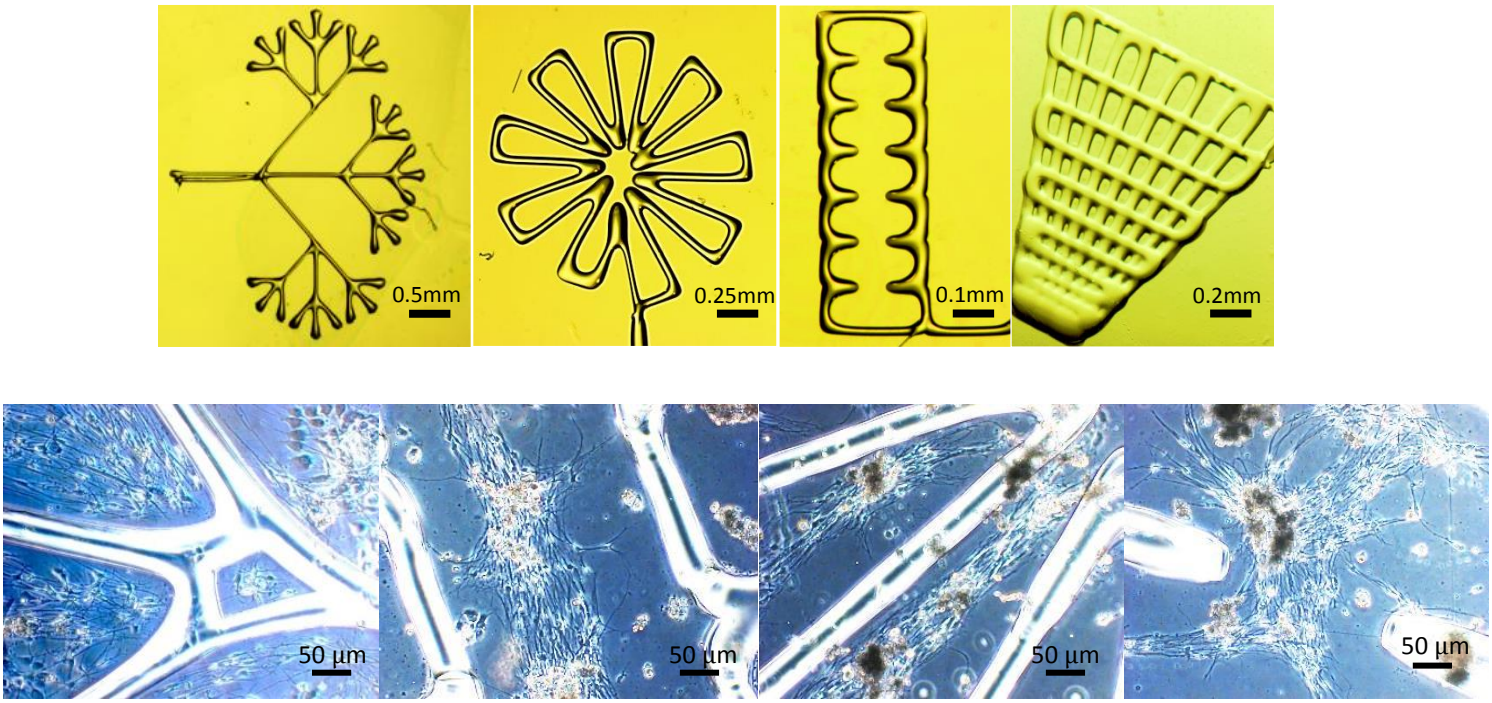

Figure S16. **DRG Cell Culture on 3D DIW Structures**. Geometric veriety of printed scaffolds (top) and DRG cell response to guidance cues of pHEMA 3D-printed scaffolds of various geometries (bottom)

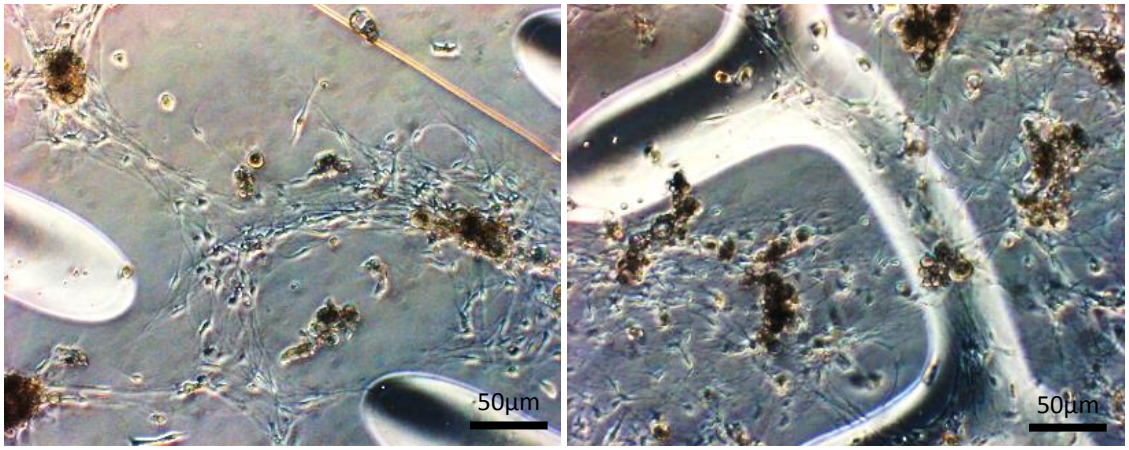

Figure S17. **Impact on Cell Attachment of Aspect Ratios and Diffusible Molecules.** Increased DRG cell attachment and process development on RGD-HEMA filaments with RGD-PDL (right) versus PDL treatment (left) on glass substrate.

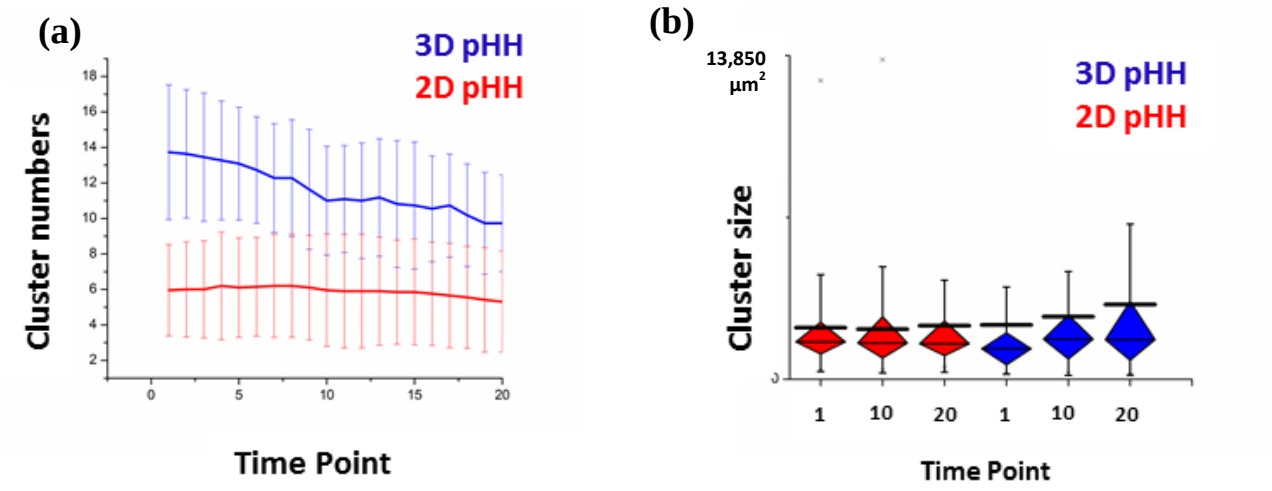

Figure S18: (a) Consolidation of clusters over time on pHH scaffolds in 2D (red) and 3D (blue). The 3D scaffold leads to a significant decrease in cell cluster numbers over time. **(b)** Box and whiskers plots showing the increase in cluster size over time facilitated by the 3D scaffolds (blue) but not the 2D scaffolds (red). The black line represents the mean, showing the (only slight) increase of overall size of clusters over time in 3D. Whiskers extend to the minima and maxima of 90% of the data. Box is divided by the median line into first quartile (bottom part) and third quartile (top part) of the data.

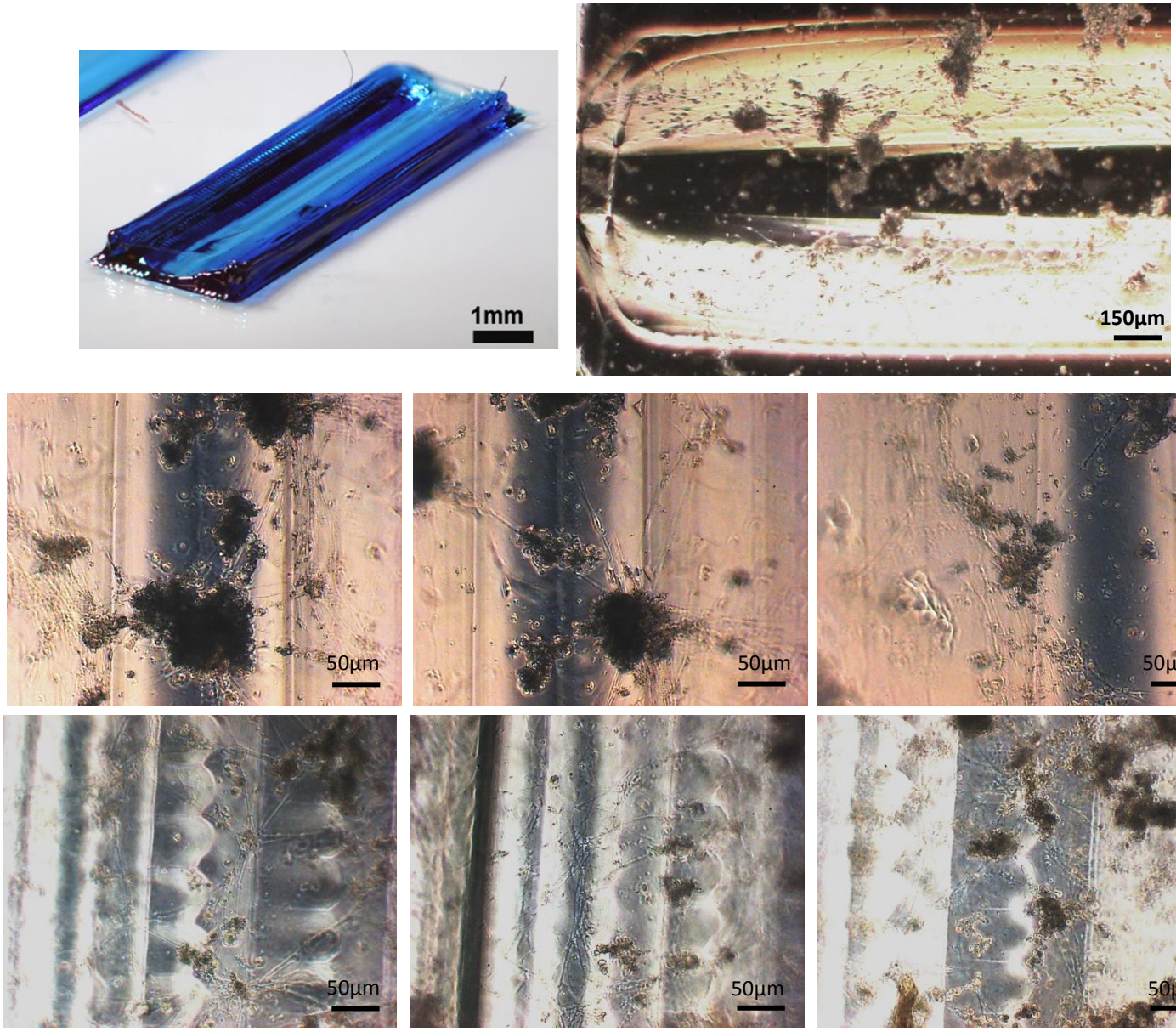

Figure S19. DRG Cell Culture Response on 3D Scaffolds. Angled view of the printed 3D scaffold before cell culture (top left); phase contrast image of DRG cell growth on a pHH 3D scaffold (top right); zoomed-in phase contrast images of cell clusters or network details on pHH (middle row) and RGD-pHH 3D scaffolds (bottom row).

Table S1. Results of Tukey's range test for morphological data - surface coverage fractions - acquired from cell cultures developed on different engineered surfaces (Figure 1)

Comparison	MeanDiff	SEM	q Value	P	Alpha	Sig	LCL	UCL
*lin*RGD-PDL I *cyc*RGD-PDL I	-84.6043	43.93858	2.72309	0.54239	0.05	0	-225.054	55.8459
cycRGD-PDL II cycRGD-PDL I	141.8669	43.93858	4.56615	0.04622	0.05	1	1.41672	282.3171
cycRGD-PDL II linRGD-PDL I	226.4712	43.93858	7.28923	1.82E-04	0.05	1	86.02099	366.9213
linRGD-PDL II cycRGD-PDL I	584.2457	43.93858	18.80462	6.94E-09	0.05	1	443.7955	724.6958
linRGD-PDL II linRGD-PDL I	668.8499	43.93858	21.5277	2.24E-09	0.05	1	528.3998	809.3001
linRGD-PDL II cycRGD-PDL II	442.3788	43.93858	14.23847	1.54E-08	0.05	1	301.9286	582.829
cycRGD-PDL III cycRGD-PDL I	407.5935	43.93858	13.11886	4.51E-08	0.05	1	267.1434	548.0437
cycRGD-PDL III linRGD-PDL I	492.1978	43.93858	15.84195	9.08E-09	0.05	1	351.7476	632.6479
cycRGD-PDL III cycRGD-PDL II	265.7266	43.93858	8.55272	1.06E-05	0.05	1	125.2765	406.1768
cycRGD-PDL III linRGD-PDL II	-176.652	43.93858	5.68575	0.00557	0.05	1	-317.102	-36.202
linRGD-PDL III cycRGD-PDL I	214.0237	43.93858	6.8886	4.39E-04	0.05	1	73.57357	354.4739
linRGD-PDL III linRGD-PDL I	298.628	43.93858	9.61168	1.10E-06	0.05	1	158.1778	439.0782
linRGD-PDL III cycRGD-PDL II	72.15685	43.93858	2.32245	0.7225	0.05	0	-68.2933	212.607
linRGD-PDL III linRGD-PDL II	-370.222	43.93858	11.91602	5.88E-08	0.05	1	-510.672	-229.772
linRGD-PDL III cycRGD-PDL III	-193.57	43.93858	6.23026	0.00181	0.05	1	-334.02	-53.1196
Glass cycRGD-PDL I	387.8839	43.93858	12.48449	5.07E-08	0.05	1	247.4337	528.334
Glass linRGD-PDL I	472.4881	43.93858	15.20757	1.17E-08	0.05	1	332.038	612.9383
Glass cycRGD-PDL II	246.017	43.93858	7.91834	4.45E-05	0.05	1	105.5668	386.4672
Glass linRGD-PDL II	-196.362	43.93858	6.32013	0.0015	0.05	1	-336.812	-55.9116
Glass cycRGD-PDL III	-19.7097	43.93858	0.63438	0.9998	0.05	0	-160.16	120.7405
Glass linRGD-PDL III	173.8601	43.93858	5.59589	0.00668	0.05	1	33.40997	314.3103
PDL cycRGD-PDL I	91.46733	43.93858	2.94398	0.44346	0.05	0	-48.9828	231.9175
PDL linRGD-PDL I	176.0716	43.93858	5.66707	0.00579	0.05	1	35.62144	316.5218
PDL cycRGD-PDL II	-50.3996	43.93858	1.62217	0.94185	0.05	0	-190.85	90.05061
PDL linRGD-PDL II	-492.778	43.93858	15.86063	9.02E-09	0.05	1	-633.229	-352.328
PDL cycRGD-PDL III	-316.126	43.93858	10.17488	4.08E-07	0.05	1	-456.576	-175.676
PDL linRGD-PDL III	-122.556	43.93858	3.94462	0.12656	0.05	0	-263.007	17.89376
PDL Glass	-296.417	43.93858	9.54051	1.27E-06	0.05	1	-436.867	-155.966

Table S2. Results of Tukey's range test for morphological data - surface coverage fractions - acquired from cell cultures developed on different engineered surfaces (Figure 2).

Comparison	MeanDiff	SEM	q Value	P	Alpha	Sig	LCL	UCL
cycRGD-PDL III cycRGD-PDL I	0.35112	0.04102	12.10397	5.82E-08	0.05	1	0.21532	0.48692
cycRGD-PDL III linRGD-PDL I	0.36737	0.04102	12.6641	5.19E-08	0.05	1	0.23156	0.50317
cycRGD-PDL III cycRGD-PDL II	0.36391	0.04102	12.5449	5.28E-08	0.05	1	0.22811	0.49971
cycRGD-PDL III linRGD-PDL II	0.32195	0.04102	11.09863	7.79E-08	0.05	1	0.18615	0.45776
linRGD-PDL III cycRGD-PDL III	-0.26874	0.04102	9.26434	1.38E-06	0.05	1	-0.40455	-0.13294
cycRGD-PDL IV cycRGD-PDL III	-0.26556	0.04102	9.15444	1.80E-06	0.05	1	-0.40136	-0.12975
linRGD-PDL IV cycRGD-PDL III	-0.30431	0.04102	10.49035	1.29E-07	0.05	1	-0.44011	-0.16851
Glass cycRGD-PDL III	-0.24708	0.04102	8.51766	8.59E-06	0.05	1	-0.38289	-0.11128
PDL cycRGD-PDL III	-0.34736	0.04102	11.97431	5.96E-08	0.05	1	-0.48316	-0.21155

Table S3. Results of Tukey's range test for morphological data - scaffold coverage fractions - acquired from cell cultures developed on different engineered surfaces (Figure 4.a, top).

Comparison	MeanDiff	SEM	q Value	P	Alpha	Sig	LCL	UCL
RGD-pHH/RGD-PDL/g-1 vs. RGD-pHH/PDL/g-1	0.13894	0.03355	5.85587	0.00289	0.05	1	0.028	0.24987
RGD-pHH/RGD-PDL/g-1 vs. pHH/RGD-PDL/g-1	0.12064	0.02122	8.03937	2.93E-06	0.05	1	0.05047	0.1908
pHH/RGD-PDL/H-1 vs. RGD-pHH/RGD-PDL/g-1	-0.11466	0.01838	8.82348	1.93E-07	0.05	1	-0.17543	-0.0539
RGD-pHH/RGD-PDL/H-1 vs. RGD-pHH/PDL/g-1	0.17102	0.03407	7.09804	7.10E-05	0.05	1	0.05836	0.28368
RGD-pHH/RGD-PDL/H-1 vs. pHH/RGD-PDL/g-1	0.15272	0.02203	9.80174	2.91E-08	0.05	1	0.07987	0.22557
RGD-pHH/RGD-PDL/H-1 vs. RGD-pHH/PDL/H-1	0.10923	0.03082	5.01202	0.02398	0.05	1	0.00733	0.21113
RGD-pHH/RGD-PDL/H-1 vs. pHH/RGD-PDL/H-1	0.14675	0.01931	10.74644	2.09E-08	0.05	1	0.0829	0.2106
RGD-pHH/RGD-PDL/g-2 vs. RGD-pHH/PDL/g-2	0.09972	0.02117	6.66139	2.81E-04	0.05	1	0.02972	0.16971
RGD-pHH/RGD-PDL/g-2 vs. pHH/RGD-PDL/g-2	0.14329	0.01894	10.69722	2.11E-08	0.05	1	0.08066	0.20593
RGD-pHH/PDL/H-2 vs. pHH/RGD-PDL/g-2	0.07591	0.01967	5.45724	0.00822	0.05	1	0.01087	0.14096
pHH/RGD-PDL/H-2 vs RGD-pHH/RGD-PDL/g-2	-0.10799	0.01708	8.94217	1.34E-07	0.05	1	-0.16446	-0.05152
RGD-pHH/RGD-PDL/H-2 vs. RGD-pHH/PDL/g-2	0.1002	0.02062	6.87264	1.46E-04	0.05	1	0.03203	0.16837
RGD-pHH/RGD-PDL/H-2 vs. pHH/RGD-PDL/g-2	0.14378	0.01833	11.09528	1.91E-08	0.05	1	0.08319	0.20437
RGD-pHH/RGD-PDL/H-2 vs. pHH/RGD-PDL/H-2	0.10848	0.01639	9.35931	4.85E-08	0.05	1	0.05428	0.16267

Table S4. Results of Tukey's range test for morphological data - scaffold coverage fractions - acquired from cell cultures developed on different engineered surfaces (Figure 4.a, bottom).

Comparison	MeanDiff	SEM	q Value	P	Alpha	Sig	LCL	UCL
RGD-pHH/RGD-PDL/H-1 vs. RGD-pHH/PDL/g-1	0.21398	0.06217	4.86769	0.03315	0.05	1	0.00844	0.41953
RGD-pHH/RGD-PDL/H-1 vs. pHH/RGD-PDL/H-1	0.11868	0.03523	4.7635	0.04155	0.05	1	0.00219	0.23518
RGD-pHH/RGD-PDL/g-2 vs. RGD-pHH/PDL/g-2	0.1383	0.03863	5.0636	0.0213	0.05	1	0.01059	0.26601
RGD-pHH/PDL/H-2 vs. pHH/RGD-PDL/g-2	-0.19091	0.03589	7.52192	1.75E-05	0.05	1	-0.30958	-0.07224
RGD-pHH/PDL/H-2 vs. RGD-pHH/RGD-PDL/g-2	-0.24507	0.04219	8.21421	1.58E-06	0.05	1	-0.38457	-0.10557
pHH/RGD-PDL/H-2 vs. RGD-pHH/PDL/H-2	0.19778	0.03263	8.57211	4.49E-07	0.05	1	0.0899	0.30567

Table S5: Comparison of mass transport behavior in pHH vs RGD- pHH 3D scaffolds. In total, we evaluated 17 regions of interest (ROIs) in pHH, and 19 ROIs in RGD-pHH.

		Mean pHH	Mean RGD-pHH	U-Test Score
Diffusion	Radial	21.88	36.62	0.93
Advection Spread	Radial	0.03	0.20	0.08
Start Spatial Scale	Radial	2.81	3.20	0.47
End Spatial Scale	Radial	3.36	4.12	0.25
Diffusion	YZ	28.82	5.62	0.27
Advection	YZ	0.05	0.06	0.75
Advection Spread	YZ	2.06	2.07	0.36
End Spatial Scale	YZ	4.32	4.16	0.80
Diffusion	XZ	3.64	4.84	0.43
Advection Spread	XZ	0.11	0.09	0.08
Start Spatial Scale	XZ	1.85	1.69	0.14
End Spatial Scale	XZ	4.06	5.19	0.08
Diffusion	YX	13.63	3.80	0.11
Advection Spread	YX	0.09	0.04	0.33
Start Spatial Scale	YX	2.37	2.06	0.10
End Spatial Scale	YX	3.16	2.72	0.16
Diffusion coefficient in 1×10^{-6} μm/s, advection spread in nm/s, spatial scales in μm				

Table S6: Comparison of mass transport behavior in pHH vs RGD-pHH 3D scaffolds, steps only. In total, there were 11 ROIs on pHH and RGD-pHH scaffolds.

		Mean pHH	Mean RGD-pHH	U-Test Score
Diffusion	radial	14.52	44.79	0.74
Advection Spread	radial	0.03	0.22	0.13
Start Spatial Scale	radial	2.59	3.20	0.31
End Spatial Scale	radial	3.07	4.09	0.24
Diffusion	YZ	35.86	4.29	0.74
Advection Spread	YZ	0.03	0.04	0.39
Start Spatial Scale	YZ	1.91	2.04	0.20
End Spatial Scale	YZ	3.77	4.13	0.15
Diffusion	XZ	4.28	6.65	0.79
Advection Spread	XZ	0.09	0.14	0.90
Start Spatial Scale	XZ	1.70	1.81	0.45
End Spatial Scale	XZ	3.90	6.75	0.09
Diffusion	YX	12.42	2.53	0.19
Advection Spread	YX	0.06	0.02	0.90
Start Spatial Scale	YX	2.23	2.02	0.37
End Spatial Scale	YX	3.09	2.58	0.45
Diffusion coefficient in 1×10−6 μm/s, advection spread in nm/s, spatial scales in μm				